Tuning the Electronic Transport Properties of Zigzag Graphene Nanoribbons via Hydrogenation Separators

ARTICLE *in* THE JOURNAL OF PHYSICAL CHEMISTRY C · DECEMBER 2011

Impact Factor: 4.77 · DOI: 10.1021/jp208892h

4 AUTHORS:

Xiao-Fei Li
University of Electronic Science and Technol…
53 PUBLICATIONS **422** CITATIONS
SEE PROFILE

Ling Wang
Fourth Military Medical University
277 PUBLICATIONS **2,113** CITATIONS
SEE PROFILE

Ke-Qiu Chen
Hunan University
158 PUBLICATIONS **2,057** CITATIONS
SEE PROFILE

Yi Luo
KTH Royal Institute of Technology
445 PUBLICATIONS **8,944** CITATIONS
SEE PROFILE

THE JOURNAL OF PHYSICAL CHEMISTRY C

ARTICLE

pubs.acs.org/JPCC

Tuning the Electronic Transport Properties of Zigzag Graphene Nanoribbons via Hydrogenation Separators

Xiao-Fei Li,[*,†,‡] Ling-Ling Wang,[†] Ke-Qiu Chen,[†] and Yi Luo[‡,§]

[†]School of Physics and Microelectronics, Hunan University, Changsha 410082, China

[‡]Department of Theoretical Chemistry, Royal Institute of Technology, S-106 91 Stockholm, Sweden

[§]Hefei National Laboratory for Physical Sciences at the Microscale, University of Science and Technology of China, 230026, Hefei, China

ABSTRACT: Hydrogenation technique is known to be useful for opening up the band gap and controlling the electronic properties of the graphene. We have demonstrated with first principles calculations that the hydrogenation can be used to make separators to electrically separate zigzag graphene nanoribbons (zGNR) and tune their transport properties. First principles calculations reveal that each hydrogenation separator can introduce two conducting edge-like states into the subbands around the Fermi level, which can greatly enhance the conductance of the system. We find that the zGNRs with hydrogenation separators are still spin polarized; the distributions of spin densities are mainly located along the two edges of the pristine nanoribbon and the borders of the separators. The current polarization shows a nice oscillation behavior as a function of the position of the separator, which originates from the symmetry dependent transport character of the zGNRs. Moreover, we find that the hydrogenation separators can screen the impact of rough edges, which makes rough-edge zGNRs behave like smooth-edge zGNRs. Our findings could be very useful for designing electronic devices based on the hydrogenation of graphene nanoribbons.

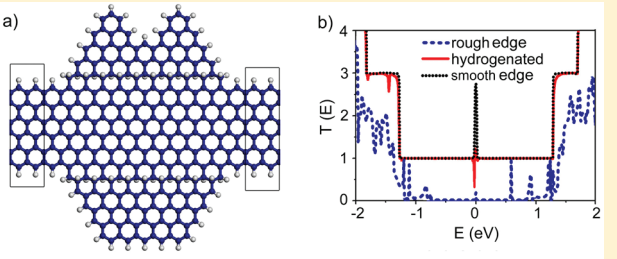

I. INTRODUCTION

The huge potential applications of the graphene in electronic devices have attracted many experimental and theoretical studies in recent years.[1−3] It is known that the electronic property of the graphene is sensitive to the defects,[3] the dopants,[4,5] the ripples on its surface,[6] the shape of its edge,[7,8] and especially its width.[9] With the reduction of the width, the graphene can change its electrical character from semimetal to semiconducting gradually.[10] Theoretical studies have shown that the graphene nanoribbons (GNRs), especially the narrow GNRs with smooth edge, possess exciting magnetic, optical, and electronic properties.[11−13] Many experimental techniques have been developed over the years to produce narrow GNRs,[14−19] ranging from the mechanical cutting[17] and the unzipping carbon nanotubes (CNT)[15] to the decomposition of C_{60}[19] or the chemical synthesis.[20] The transport measurements on the produced GNRs have shown that the transport gap of narrow ribbons are much larger than that predicted by theory, while the wider ribbons have much smaller gaps than expected.[21,22] Sols et al.[23] argued that the fabrication of the narrow GNR gives rise to very rough edges breaking the GNR into a series of quantum dots, which makes the energy gap show no dependence on the orientation (i.e., zigzag or armchair direction) as required by the theory.[10,24] Thus, it is still a considerable challenge to produce narrow GNRs with smooth edges in large scale.[25]

Because of its unusual structural and electronic flexibility, graphene can be tailored by edge modifications,[26] surface physorptions,[27] substrate effects[28] or chemical functionalizations,[29] in particular, by fluorination[30,31] and hydrogenation.[32,33] Recently, Balog et al.[32] and Elias et al.[33] discovered that through the hydrogenation process it is possible to open up the band gap and control the electronic properties of the graphene. Xiang et al.[34] demonstrated that the narrow GNRs could be obtained from wider GNRs by gradually hydrogenating the edge regions. They also found that during the hydrogenation process, hydrogen atoms prefer to extend along the zigzag carbon atom chains and form thermodynamically stable 1D separators.[35] Ao et al. have investigated[36] the energy barriers for the diffusion of hydrogen atoms in graphene/graphane[37] nanoribbon heterojunctions and found that the H atoms at the interface are quite thermally stable. Wang et al. proposed a two-step-combinational approach,[38] a strain-engineered pattern to form graphene nanoripples and the curvature-directed self-assembly of H adsorption, to control the structure and the morphology of the hydrogenation separators. Such separators could be electrically insulating, can be used to define narrow GNRs in large graphene sheet, and can be used to screen the effect of rough edges. By taking advantage of the unique feature of the hydrogenation separator, we have designed by the first principles methods a series of zigzig-GNR (zGNR) based electronic devices with hydrogenation separators of different

Received: September 15, 2011
Revised: October 31, 2011
Published: November 01, 2011

sizes and positions that can effectively tune the conductance and the current polarization of the devices.

II. MODELS AND CACULATION METHODS

It is well-known that hydrogen atoms can chemically adsorb on the top of carbon atoms in graphene to construct three types of hydrogenated graphene structures: chair, boat, and washboard graphane.[39−41] By considering arbitrary boundary conditions, Akhmerov and Beenakker[42] proposed that the behavior of the zigzag edges is the most generic for the experimentally fabricated graphene nanoribbons. Considering their proposition, we have first considered the hydrogenation of a 24-zigzag-lines-wide zGNRs (24-zGNR) with the smooth edges terminated by hydrogen atoms. A cubic supercell that consists of 11 cells of 24-zGNR (528 carbon atoms are included) are used as the central scattering region of the devices (see Figure 1). At the middle of the supercell, one or two zigzag-lines of carbon atoms can be fully hydrogenated to form hydrogenated-separator, the produced devices can be denoted as (n)-H or (n,m)-H, respectively, where *n* and *m* denote the *n*th and the *m*th zigzag-line of the carbon atoms across the ribbon width are fully hydrogenated, respectively. Eight devices (9)-H, (9,10)-H, (9,11)-H, (9,12)-H, (9,13)-H, (9,14)-H, (9,15)-H, and (9,16)-H are considered in our calculations. And then we have explored the screening effect of the hydrogenation separators on the rough edges of a imperfect 6-zGNR. The electronic structures and geometrical relaxations are calculated by using Vienna ab initio simulation package (VASP-5.2)[43] with Perdew−Burke−Ernzerhof (PBE) formulation of the generalized gradient approximation (GGA) exchange−correlation functional. During the relaxation, a vacuum layer of 16 Å was used in the direction perpendicular to the graphene ribbon to avoid the artificial coulomb interaction between the contents in two neighboring cells. Two cells of the surface atoms of left and right semi-infinite electrodes were included in the scattering region to ensure all the screening effects are included into the contact region and the potential at the boundary can be found to be the same as that of the electrodes. The kinetic energy cutoff of 500 eV was employed for the plane-wave set. And the k-point meshes in the Brillouin zone (BZ) were sampled by 1 × 1 × 23 grids. All atoms were fully relaxed until the atomic forces were smaller than 0.02 eV/Å. After the structural optimizations, we found that the zGNR is largely changed its initial planar structure by the hydrogenation, a step-like separator with a step-height about 0.73 Å is formed at the hydrogenation region. The bonding length between two hydrogenated carbon atoms or between one hydrogenated and one unhydrogenated carbon atoms is about 1.54 or 1.510 Å, and the bond angle of C−C−C or C−C−H is about 109.37or 108.19°, respectively. They are very close to the corresponding structural parameters in a diamond. Each carbon atom in the separator is almost sp^3 hybridized, the four electrons in the outer shell of the carbon atom are involved in forming σ bonds. It should be mentioned that GGA-PBE is difficult to give out a reasonable structure of polyacetilene (PA)[53] and fails in optimizing of the layer-distance of graphene. However, it provides a good balance between simplicity and accuracy, and has been widely used in the studies on graphene-based systems.[20−25,51−55] On the basis of the general performance of VASP for many systems, we believe that the approach implemented in VASP should give reasonable predictions.

The electron transport properties of the zGNR devices are calculated using the ATK package,[44] which adopts a nonequilibrium Green's function method (NEGF) in combination with

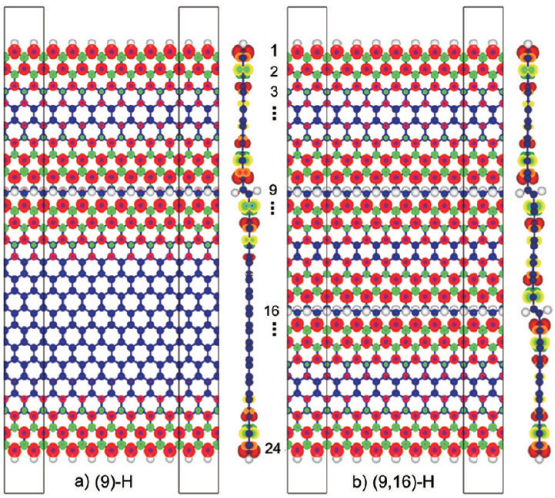

Figure 1. Spin density isosurfaces (isovalue = 0.001) of 24-zGNR with one line (a) or two lines of zigzag carbon atoms fully hydrogenated (b), the spin-up and spin-down are denoted with red and green colors, respectively. The atoms in the two rectangles are the surface atoms of left and right electrodes. The side view is also given. In the figures, carbon and hydrogenation atoms are represented by blue and white spheres, respectively.

gradient corrected density functional theory (DFT). During the transport calculations, generalized gradient approximation (GGA) with the PBE exchange-correlation functional are used. A cutoff energy of 150 Ry and a Monkhorst-Pack *k*-mesh of 1 × 1 × 100 are chosen to achieve the balance between calculation efficiency and accuracy. A double-ζ polarized (DZP) basis set is adopted for electron wave function. The spin dependent currents are calculated using Landauer−Buttiker[45] formula: $I_{\alpha\beta} = (e/h) \int_{\mu_R}^{\mu_L} T_{\alpha\beta}(E,V_b)$-$[f_L(E,V_b) - f_R(E,V_b)]\, dE$, where e is the electron charge and h is the Planck constant. $f_{L(R)}(E,V_b) = n_F(E,\mu_{L(R)})$. n_F and $\mu_{L(R)}$ are the Fermi function and the electrochemical potential of the left (right) electrodes, respectively. $T_{\alpha\beta}(E,V_b)$ is the spin-resolved transmission defined as $T_{\alpha,\beta}(E,V_b) = \mathrm{Tr}[\mathrm{Im}\{\Sigma^{\gamma}_{L_{\alpha\beta}}(E,V_b)\} G^{\gamma}_{\alpha,\beta}(E,V_b) \times \mathrm{Im}\{\Sigma^{\gamma}_{R_{\alpha\beta}}(E,V_b)\} G^{\gamma}_{\alpha,\beta}(E,V_b)]$, where $\Sigma^{r}_{L(R)}$ is the retarded self-energy matrix which takes into account the left and right electrodes. $G^{r(a)}$ is the retarded (advanced) Green's function matrix. The NEGF-DFT self-consistency was controlled by a numerical tolerance of 10^{-5} eV, and the electron temperature is set to 300 K in the transport calculations.

III. RESULTS AND DISCUSSION

Edge-Like States. Due to the sp^3 hybridized character, the hydrogenation can largely open up the energy gap of graphene and effectively separate the GNR into sub-GNRs.[32−39,46−49] Accurate calculations using GW approximation show that a fully periodically hydrogenated graphene (graphane) is a insulator,[46] while a half-hydrogenated graphene is a semiconductor with a narrow energy gap of 0.43 eV,[50] which is also the value of the experimentally observed one[39] for a special patterned graphene with hydrogen adsorption. For the graphene nanoribbons, it is known that armchair GNRs (aGNRs) and zGNRs have very different electronic structures; the aGNRs are semiconductor with the width (N) dependent energy gap and the zGNRs are metallic with peculiar edge states.[7−12] It is known that the zGNRs have spin ordering states along both edges; the relative spin orientation

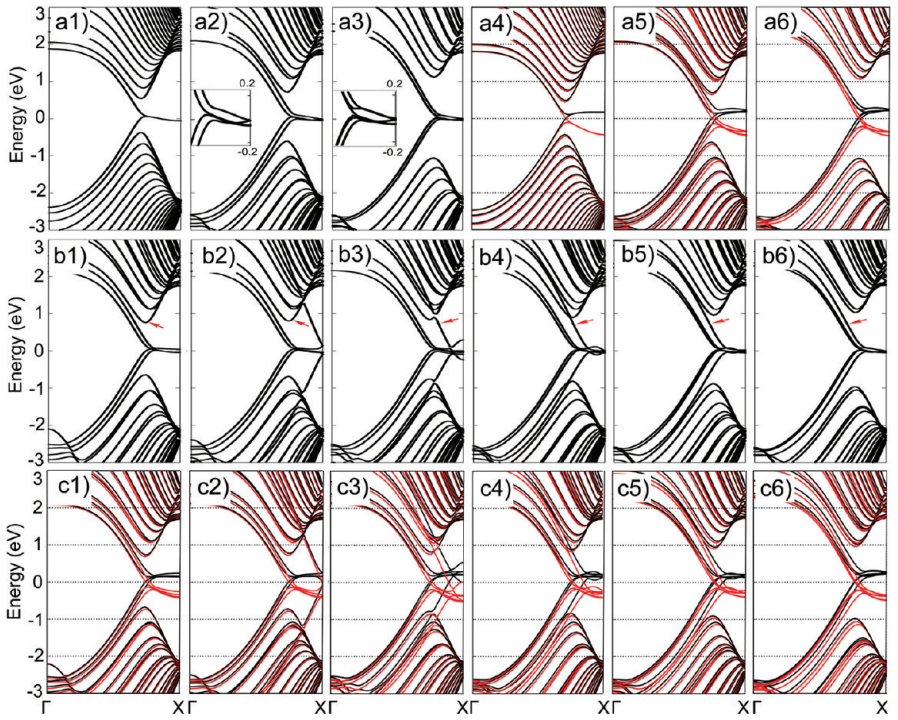

Figure 2. (a1, a2 and a3) Unpolarization band structures of devices ideal 24-zGNR, (9)-H, and (9,16)-H, respectively, and (a4, a5, and a6) polarization band structures of the corresponding devices. (b1−b6) Unpolarization band structures of devices (9,10)-H, (9,11)-H, (9,12)-H, (9,13)-H, (9,-14)-H, (9,15)-H, and (9,16)-H, respectively, and (c1−c6) polarization band structures of the corresponding devices.

between both edges can be either parallel or antiparallel. The parallel spin configuration (ferromagnetic, FM) has slightly higher energy than the antiparallel spin configuration (antiferromagnetic, AFM), and a narrow band gap can be opened in AFM state. With the presence of an external magnetic field, the ground state is found to be the FM state and the band gap is zero. Thus, in our polarization calculations, we only considered the FM state; that is, the initial spin configuration is parallel along the edges. After the spin-dependent structural relaxations, we find that all the systems still possess spin-up polarization character. As examples, the spin density isosurfaces of the device (9)-H and (9,16)-H are give in the Figure 1, panels a and b, respectively. It can be clearly seen that the spin densities distribute on the edges of the pristine zGNR and the borders along the hydrogenation separator. It looks like that one zigzag-line of fully hydrogenated carbon atoms can separate the 24-zGNR into two sub-zGNRs, and two separated hydrogenation separators could separate the 24-zGNR into three sub-zGNRs. Each separator can induce two spin-polarized edge-like states to the system. The induced states are high delocalized and quite conductive, it suggests that the hydrogenation technique could be very useful for enhancing the conductance of the GNRs. Figure 2 exhibits the band structures of the devices. The unpolarization band structure of device 24-zGNR, (9)-H, and (9,16)-H are plotted in Figure 2, panels a1, a2, and a3, whereas their polarization band structures are plotted in panels a4, a5, and a6, respectively. One can find in Figure 2, panels a1 and a4, that our calculated band structures (polarization and unpolarization) of ideal zGNR are quite similar as that from other groups,[7−12] it suggests that the GGA-PBE approach we used gives reasonable electronic structures of zGNR systems. From the other panels in Figure 2, one can find that one or two hydrogenation separators cannot open the band gap of the ideal 24-zGNR at all, but they indeed introduce conducing edge-like states into the subbands near the Fermi level of the system. The energy and the polarization feature of the edge-like states are quite similar to the real edge states. From panels a2 and a3 of Figure 2, one can clearly see that there exists two edge-like states in the device (9)-H, but there are four edge-like states in the device (9,16)-H. This means that each hydrogenation separator can introduce two edge-like states to the system. In order to examine the effect of interaction between the two separators on the introduced edge-like states, we calculated the unpolarization and polarization band structures of the devices (9,m)-H (where the m can vary from 10 to 15), the obtained results are given in Figure 2, panels b1−b6 and c1−c6, respectively. One can find that panel b1 is quite like panel a2. This can be well understood by the fact that just like in the device (9)-H, there only exists one separator in device (9,10)-H. Because the two hydrogenated carbon atom chains (the 9th and 10th zigzag lines) are connect to each other and produce a two zigzag-lines wide hydrogenation separator. It suggests that no matter how wide the hydrogenation separator is, one hydrogenation separator can only introduce two edge-like states into the system, whereas in device (9,11)-H, the two hydrogenation carbon atom chains are separated by an unhydrogenated carbon atom chain, which produces two separators. The interaction between the two separators could be large due to the short distance between them, thus the two introduced states are largely separated in figure b2). With the increase of the *m*, the second separator moves away from the first separator gradually, the interaction between them becomes smaller, and the coupling between the conducting subbands near Fermi level should be weaker, which leads the two introduced states close to the edge states of the 24-zGNR and finally become conducting edge-like states in device (9,15)-H and (9,16)-H. Thus, we can conclude that a fully hydrogenated zigzag

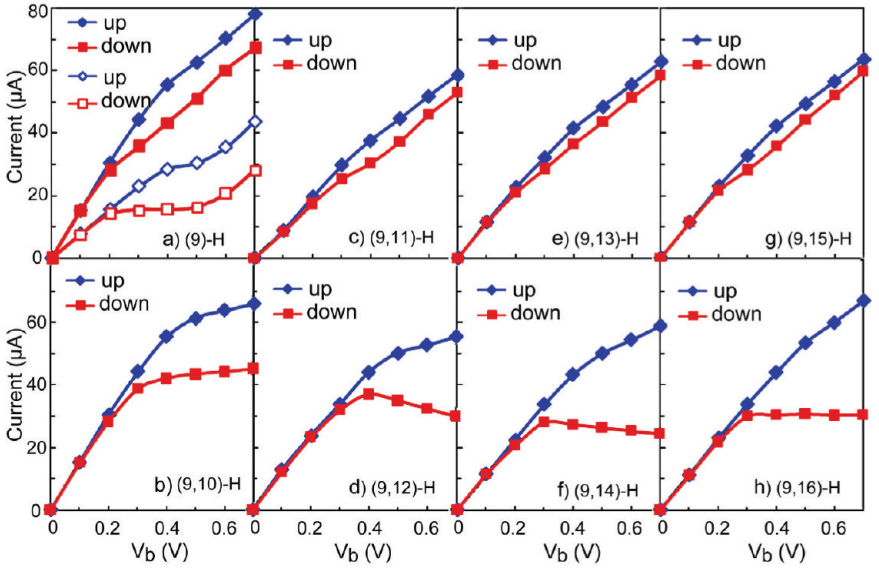

Figure 3. Spin-dependent currents of device (9)-H (a), (9,10)-H (b), (9,11)-H (c), (9,12)-H (d), (9,13)-H (e), (9,14)-H (f), (9,15)-H (g), and (9,16)-H (h), respectively. The spin-up current and spin-down current of 24-zGNR are also plotted in figure a), and denoted by the hollow diamond and the hollow square, respectively. For comparing, the currents shown in panels a and b are magnified twice.

carbon atom chain can act as a separator to electrically separate a z-GNR into two sub-GNRs, it can introduce two conducting spin-polarized edge-like states at the subbands near the Fermi level and enhance the conductance of the system. When the distance between the separators is large enough, each separator can introduce two edge-like states to the system. Most importantly, the edge-like states should originate from the insulating feature of the hydrogenation separators. The unique character of the hydrogenation separator we have found could be very useful for designing electrical devices in large graphene sheets.

Oscillation of the Current Polarization. In order to evaluate the realistic enhancing effect of the hydrogenation separators, we calculated the spin-dependent current−voltage ($I-V$) characteristics of the systems. The results are given in Figure 3, noticing in panels a and b that the current of 24-zGNR, (9)-H, and (9,10)-H are magnified twice for comparing. One can find at the low bias region (for an example, $V_b < 0.2$ V) that the conductance of the device (9,10)-H and (9)-H are almost the same, and they are about twice as that of the ideal 24-zGNR. Suggested that one hydrogenation separator can indeed double the conductance of the pristine zGNR. For the other devices, one can find that their conductance are larger than that of the device (9)-H and (9,10)-H, due to two separators are respectively included in the systems, whereas at the higher bias region, one can find that the spin current of the devices are polarized. The current polarization (ξ) can be defined with

$$\xi = \frac{I_\alpha - I_\beta}{I_\alpha + I_\beta} \qquad (2)$$

where α and β denote majority and minority spins, respectively. It is worth noticing that the current polarization of (9,10)-H is much larger than that of (9)-H, although they both include only one separator and have similar band structures (as shown in Figure 2, panels a2 and b1). The same thing happens for the other devices which included two hydrogenation separators. One can see that the current polarization is small in device (9,11)-H, (9,13)-H, and (9,15)-H, whereas it is large in the device (9,12)-H, (9,14)-H, and (9,16)-H. The current polarization presents a nice oscillation behavior as a function of the position of the second separator. The oscillation behavior of the current polarization observed here is very unique and to the best of our knowledge it has never been reported before.

In order to well understand the oscillation behavior of the current polarization, we have given the spin-dependent transmission spectra $T(E, V_b)$ of the device (9,11)-H, (9,12)-H, (9,13)-H, (9,14)-H, (9,15)-H, and (9,16)-H at the bias V_b = 0.6 V in Figure 4, panels a−f, respectively. One can find in the figure that the spin-up and spin-down transmissions are quite different near the Fermi level, suggesting the polarization occurs at the edge states and edge-likes states. The spin dependent transmission spectra also show a nice oscillation behavior with the movement of the second separator from the 10th to the 16th zigzag-line in the 24-zGNR. For examples, the minimum of the spin-down transmissions in device (9,11)-H, (9,13)-H, and (9,15)-H is almost 1, while it is almost zero in device (9,12)-H, (9,14)-H, and (9,16)-H, respectively. The similar situation can also be found in the spin-up transmission spectra. This means that the oscillation behavior of the current polarization originates in the oscillation polarization behavior of the edge (edge-like) states. It was argued[13] that although all smooth-edge zGNRs have similar band structures, they can have distinctly different transport behaviors under biases, depending on their structural symmetry. The difference arises from the different coupling between the conducting subbands around the Fermi level. In our designed systems, the (9)-H can be regarded as a device composed by two sub-zGNRs with mirror symmetry as shown in Figure 1a, whereas the device (9,10)-H is a composition of two sub-zGNRs one with mirror symmetry and one with asymmetry. The difference of the symmetry between the sub-zGNRs in device (9)-H and (9,10)-H allows a different coupling between the conducting edge (edge-like) states around the Fermi level, which leads to a distinct spin-dependent transmission and thus the difference of the current polarization in these two devices. With the hydrogenation moving from the 10th to the 11th zigzag line, the produced device

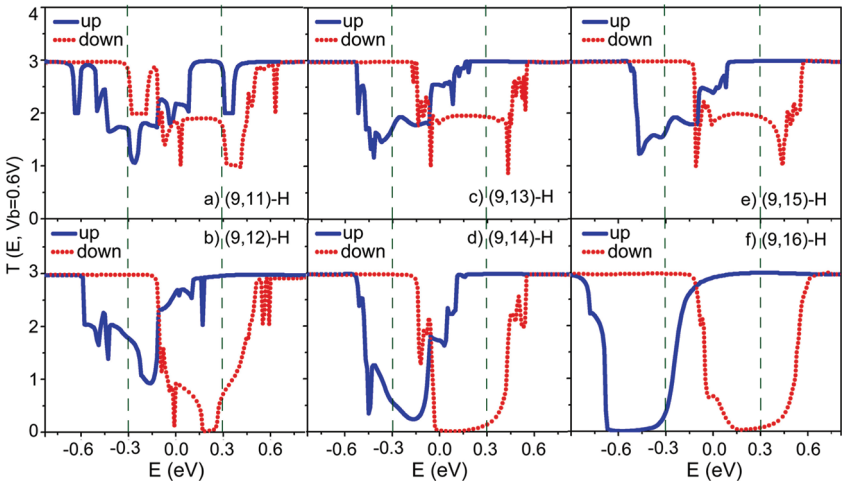

Figure 4. Spin-dependent transmission spectra $T(E,V_b)$ of the device (9,11)-H (a), (9,12)-H (b), (9,13)-H (c), (9,14)-H (d), (9,15)-H (e), and (9,16)-H (f) at the bias V_b = 0.6 V.

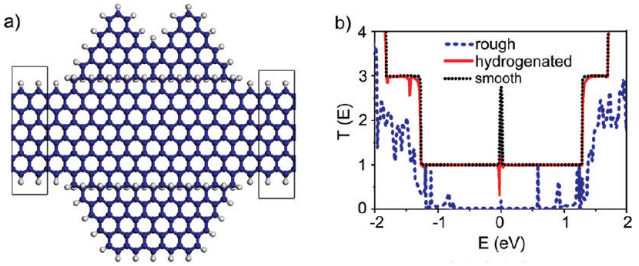

Figure 5. (a) Optimized scattering region of the a rough-edge device, along the smooth edges of 6-zGNR electrodes, two zigzag-lines of carbon atoms are fully hydrogenated to form separators. (b) Zero-bias transmissions spectra T(E) of the smooth-edge 6-zGNR (dotted line), the rough-edge device (dashed line), and the rough-edge device with hydrogenation separators (solid line), respectively.

(9,11)-H includes two separators, which separate the 24-zGNR into three sub-zGNRs. With the second separator moving from the 11th to the 16th gradually, the first sub-zGNR remains its mirror symmetry unchanged, while the symmetries of the other two sub-zGNRs are changed oscillatorily. This directly results in the oscillations of current polarization.

Screening Rough Edges. It is known that, the fabricated GNRs at present always have rough edges at the both sides, the rough edges have a significant impact on the electronic structures and the transport properties of GNR based devices.[20−25] We have found that the impact of the rough edges can be perfectly screened by the hydrogenation separators.

The device we used is a rough-edge 6-zGNR as shown in Figure 5a, along the smooth edges of the perfect 6-zGNR electrodes, two zigzag-lines of carbon atoms can be fully hydrogenated to form separators. The calculated zero-bias transmissions $T(E)$ the rough-edge device with or without the hydrogenation separators are given in Figure 5b, the transmission of the smooth-edge 6-zGNR is also given for comparison. One can see in the figure that the perfect 6-zGNR has a unit transmission around the Fermi level and a high transmission peak right at the Fermi level, indicating the high conductivity of the smooth edges system, while for the rough-edge device, one can see that the transmission is almost zero around the Fermi level, confirmed the strong

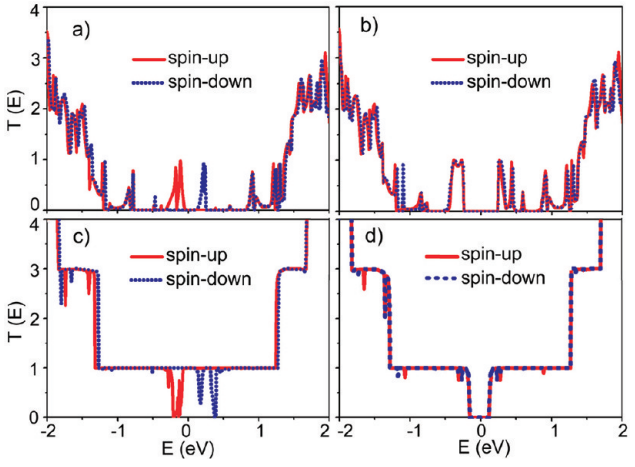

Figure 6. Zero-bias transmission $T(E)$ of the rough-edge device under FM state (a) and AFM state (b), and the zero-bias transmission $T(E)$ of the rough-edge device including hydrogenation separators under FM state (c) and AFM state (d), respectively.

impact of rough edges on the conductivity of the zGNR. With the presence of the hydrogenated separators at each side, one can see that the transmission curve of the device coincides with that of the smooth edges system very well. This suggests that the impact of rough edges can be totally screened by the hydrogenation separators. We have also calculated the spin-dependent transmissions of the rough-edge device, both FM state and AFM state are considered, and the obtained results are plotted in Figure 6, panels a (FM state) and b (AFM state), respectively. For the device including hydrogenation separators, the obtained results are plotted in Figure 6, panels c (AF state) and d (AFM state), respectively. One can find in the figure that the conductance of the rough edges system is poor, there only exists several transmission peaks around the Fermi level. With the presence of hydrogenation separators, a transmission platform with a strength of "1" presents around the Fermi level, suggesting a high conductance of the system and the ballistic electronic transport character. Normally speaking, ballistic electronic transports only present in perfect GNRs with smooth edges. This means that the hydrogenation

separators can perfectly screen the impact of the rough edges and make the rough-edge zGNRs behave like smooth-edge zGNRs.

IV. SUMMARY

We have applied first principles methods to study the effect of hydrogenation on the electronic structures and transport properties of a zigzag graphene nanoribbon. It is found that the hydrogenation can be also used to make separators to electrically separate a wide zigzag graphene nanoribbon into narrow zigzag graphene nanoribbons, when the distance between the separators is wide enough, each of them can introduce two conducting edge-like states into the subbands around the Fermi level, which can highly enhance the conductance of the system. We find that the system with separators is still polarized; the spin dependent densities mainly distribute on the two edges of the pristine nanoribbon and the borders along the hydrogenated zigzag lines. The current polarization shows a nice oscillation behavior with the movement of the separator, which originates from the symmetry-dependent transport properties of zigzag graphene nanoribbons. We have also investigated the screening effect of the hydrogenation separator in detail. We find that the hydrogenation separator can totally screen the impact of rough edges, which makes the rough-edge zGNRs behave like smooth-edge zGNRs. Our findings could be very useful for designing electronic devices based on the hydrogenation of the graphene sheets.

AUTHOR INFORMATION

Corresponding Author
*E-mail: xfli@kth.se.

ACKNOWLEDGMENT

We acknowledge supports from Swedish Research Council (VR), Swedish National Infrastructure for Computing (SNIC), Goran Gustaffson Foundation for Research in Natural Sciences and Medicine, Natural Science Foundation of China (Grant Nos. 20925311, 60871065, and 61176116), Ministry of Science and Technology of China (Grant No. 2010CB923300), and China Scholarship Council (CSC).

REFERENCES

(1) Novoselov, K. S.; Geim, A. K.; Morozov, S. V.; Jiang, D.; Zhang, Y.; Dubonos, S. V.; Gregorieva, I. V.; Firsov, A. A. *Science* **2004**, *306*, 666.
(2) Geim, A.; Novoselov, K. *Nat. Mater.* **2007**, *6*, 183.
(3) Castro Neto, A. H.; Guinea, F.; Peres, N. M. R.; Novoselov, K. S.; Geim, A. K. *Rev. Mod. Phys.* **2009**, *81*, 109.
(4) Biel, B.; Blase, X.; Triozon, F.; Roche, S. *Phys. Rev. Lett.* **2009**, *102*, 096803.
(5) Boukhvalov, D. W.; Katsnelson, M. I. *Nano Lett.* **2008**, *8*, 4373.
(6) Bao, W.; Miao, F.; Chen, Z.; Zhang, H.; Jang, W.; Dames, C.; Lau, C. N. *Nat. Nanotechnol.* **2009**, *4*, 562.
(7) Guinea, F.; Horovitz, B.; Le Doussal, P. *Phys. Rev. B* **2008**, *77*, 205421.
(8) Kan, E.; Li, Z. Y.; Yang, J. L.; Hou, J. G. *J. Am. Chem. Soc.* **2008**, *130*, 4224.
(9) Han, M. Y.; Öezyilmaz, B.; Zhang, Y.; Kim, P *Phys. Rev. Lett.* **2007**, *98*, 206805.
(10) Barone, V.; Hod, O.; Scuseria, G. E. *Nano Lett.* **2006**, *6*, 2748.
(11) Das Sarma, S.; Adam, S.; Hwang, E. H.; Rossi, E. *Rev. Mod. Phys.* **2011**, *83*, 407.
(12) Peres, N. M. R. *Rev. Mod. Phys.* **2011**, *82*, 2673.
(13) Li, Z.; Qian, H.; Wu, J.; Gu, B.-L.; Duan, W. *Phys. Rev. Lett.* **2008**, *100*, 206802.
(14) Park, S.; Ruoff, R. S. *Nat. Nanotechnol.* **2009**, *4*, 217.
(15) Jiao, L.; Zhang, L.; Wang, X.; Diankov, G.; Dai, H. *Nature* **2009**, *458*, 877.
(16) Kim, K. S.; Zhao, Y.; Jang, H.; Lee, S. Y.; Kim, J. M.; Kim, K. S.; Ahn, J. H.; Kim, P.; Choi, J. Y.; Hong, B. H. *Nature* **2009**, *457*, 706.
(17) Campos, L. C.; Manfrinato, V. R.; Sanchez-Yamagishi, J. D.; Kong, J.; Jarillo-Herrero, P. *Nano Lett.* **2009**, *9*, 2600.
(18) Dato, A.; Radmilovic, V.; Lee, Z.; Phillips, J.; Frenklach, M. *Nano Lett.* **2008**, *8*, 2012.
(19) Perdigão, L. M. A.; Sabki, S. N.; Garfitt, J. M.; Capiod, P.; Beton, P. H. *J. Phys. Chem. C* **2011**, *115* (15), 7472–7476.
(20) Cai, J.; Ruffieux, P.; Jaafar, R.; Bieri, M.; Braun, T.; Blankenburg, S.; Muoth, M.; Seitsonen, A. P.; Saleh, M.; Feng, X.; Müllen, K.; Fasel, R. *Nature* **2010**, *466*, 470.
(21) Guinea, F.; Horovitz, B.; Le Doussal, P. *Phys. Rev. B* **2008**, *77*, 205421.
(22) Sols, F.; Guinea, F.; Castro Neto, A. H. *Phys. Rev. Lett.* **2007**, *99*, 166803.
(23) Berashevich, J; Chakraborty, T *Phys. Rev. B* **2010**, *82*, 134415.
(24) Huard, B.; Sulpizio, J. A.; Stander, N.; Todd, K.; Yang, B.; Goldhaber-Gordon, D. *Phys. Rev. Lett.* **2007**, *98*, 236803.
(25) Jia, X.; Campos-Delgado, J.; Terrones, M.; Meunier, V.; Dresselhaus, M. S. *Nanoscale* **2011**, *3*, 86.
(26) Kan, E.; Li, Z. Y.; Yang, J. L.; Hou, J. G. *J. Am. Chem. Soc.* **2008**, *130*, 4224.
(27) Lu, Y. H.; Chen, W.; Feng, Y. P. *J. Phys. Chem. B* **2009**, *113* (1), 2–5.
(28) Huang, L.; Hartland, G. V.; Chu, L.-Q.; Luxmi; Feenstra, R. M.; Lian, C.; Tahy, K.; Xing, H. *Nano Lett.* **2010**, *10*, 1308. Gao, B.; Hartland, G.; Fang, T.; Kelly, M.; Jena, D.; Xing, H. G.; Huang, L. *Nano Lett.* **2011**, *11*, 3184.
(29) Prezhdo, O. V.; Kamat, P. V.; Schatz, G. C. *J. Phys. Chem. C* **2011**, *115* (8), 3195–3197. Suggs, K.; Reuven, D.; Wang, X.-Q. *J. Phys. Chem. C* **2011**, *115* (8), 3313–3317.
(30) Yang, H.; Chen, M.; Zhou, H.; Qiu, C.; Hu, L.; Yu, F.; Chu, W.; Sun, S.; Sun, L. *J. Phys. Chem. C* **2011**, *115* (34), 16844–16848.
(31) Tang, S.; Zhang, S. *J. Phys. Chem. C* **2011**, *115* (33), 16644–16651.
(32) Balog, R.; Jorgensen, B.; Nilsson, L.; Andersen, M.; Rienks, E.; Bianchi, M.; Fanetti, M.; Laegsgaard, E.; Baraldi, A.; Lizzit, S.; Slijivancanin, Z.; Besenbacher, F.; Hammer, B.; Pedersen, T. G.; Hofmann, P.; Hornekaer, L. *Nat. Mater.* **2010**, *9*, 315.
(33) Elias, D. C.; Nair, R. R.; Mohiuddin, T. M. G.; Morozov, S. V.; Blake, P.; Halsall, M. P.; Ferrari, A. C.; Boukhvalov, D. W.; Katsnelson, M. I.; Geim, A. K.; Novoselov, K. S. *Science* **2009**, *323*, 610.
(34) Xiang, H.; Kan, E.; Wei, S.-H.; Whangbo, M.-H.; Yang, J. *Nano Lett.* **2009**, *9*, 4025.
(35) Xiang, H. J.; Kan, E. J.; Wei, S.-H.; Gong, X. G.; Whangbo, M.-H. *Phys. Rev. B* **2010**, *82*, 165425.
(36) Ao, Z. M.; Hernández-Nieves, A. D.; Peeters, F. M.; Li, S. *Appl. Phys. Lett.* **2010**, *97*, 233109.
(37) Lu, Y. H.; Feng, Y. P. *J. Phys. Chem. C* **2009**, *113* (49), 20841–20844.
(38) Wang, Z. F.; Zhang, Y.; Liu, F. *Phys. Rev. B* **2011**, *83*, 041403.
(39) Ruoff, R. *Nat. Nanotechnol.* **2008**, *3*, 10.
(40) Sofo, J. O.; Chaudhari, A. S.; Barber, G. D. *Phys. Rev. B* **2007**, *75*, 153401.
(41) Artyukhoy, V. I.; Chernozatonskii, L. A. *J. Phys. Chem. A* **2010**, *114* (16), 5389.
(42) Akhmerov, A. R.; Beenakker, C.W. J. *Phys. Rev. B* **2008**, *77*, 085423.
(43) Kresse, G.; Furthmüller, J. *Phys. Rev. B* **1996**, *54*, 11169. Perdew, J. P.; Burke, K.; Ernzerhof, M. *Phys. Rev. Lett.* **1996**, *77*, 3865.
(44) Brandbyge, M.; Mozos, J.-L.; Ordejón, P.; Taylor, J.; Stokbor, K. *Phys. Rev. B* **2002**, *65*, 165401.
(45) Buttiker, M.; Imry, Y.; Landauer, R.; Pinhas, S. *Phys. Rev. B* **1985**, *31*, 6207. Buttiker, M. *Phys. Rev. Lett.* **1986**, *57*, 1761.

(46) Lebègue, S.; Klintenberg, M.; Eriksson, O.; Katsnelson, M. I. *Phys. Rev. B* **2009**, *79*, 245117.
(47) Bostwick, A.; McChesney, J. L.; Emtsev, K. V.; Seyller, T.; Horn, K.; Kevan, S. D.; Rotenberg, E. *Phys. Rev. Lett.* **2009**, *103*, 056404.
(48) Boukhvalov, D. W.; Katsnelson, M. I.; Lichtenstein, A. I. *Phys. Rev. B* **2008**, *77*, 035427.
(49) Wu, D. D.; Jiang, F.; Yin, G.; Chen, H.; Liang, Y. Y.; Mizuseki, H.; Kawazoe, Y. *J. Appl. Phys.* **2011**, *110*, 033712.
(50) Zhou, J.; Wu, M. M.; Zhou, X.; Sun, Q. *Appl. Phys. Lett.* **2009**, *95*, 103108.
(51) Kan, E.; Li, Z.; Yang, J.; Hou, J. G. *Appl. Phys. Lett.* **2007**, *91*, 243116.
(52) Hod, O.; Barone, V.; Scuseria, E. G. *Phys. Rev. B* **2008**, *77*, 035411.
(53) Ramírez-Solís, A.; Kirtman, B.; Bernal-Jáquez, R.; Zicovich-Wilson, C. M. *J. Phys. Chem. C* **2008**, *112* (25), 9493.
(54) Casolo, S.; Flage-Larsen, E.; Løvvik, O. M.; Darling, G. R.; Tantardini, G. F. *Phys. Rev. B* **2010**, *81*, 205412.
(55) Huang, P.; Carter, E. A. *Annu. Rev. Phys. Chem.* **2008**, *59*, 261.